

RAL 93067

R61 RR COPY 2

ACCN: 220502

RAL-93-067

Science and Engineering Research Council

# Rutherford Appleton Laboratory

Chilton DIDCOT Oxon OX11 0QX

RAL-93-067

## An Introduction to Magnetic Photon Scattering

D Kechrakos S W Lovesey and K N Trohidou

September 1993

**Science and Engineering Research Council**

"The Science and Engineering Research Council does not accept any responsibility for loss or damage arising from the use of information contained in any of its reports or in any communication about its tests or investigations"

**An Introduction to**  
**MAGNETIC PHOTON SCATTERING**

**Studies of condensed matter**

D. Kechrakos<sup>+</sup>, S. W. Lovesey<sup>\*</sup>, and K. N. Trohidou<sup>+</sup>

<sup>+</sup> NCSR "Democritos", P.O. Box 60228, GR-153 10 Aghia  
Paraskevii, Greece.

<sup>\*</sup> Rutherford Appleton Laboratory, Oxfordshire OX11 0QX, U.K.

Dedicated to Prof. E. F. Bertaut on the occasion of his 80th birthday.

Received: July 2, 1993;

Photon scattering, magnetic materials

**Abstract**

A brief survey is provided of some recent developments in the application of photon beams to study magnetic properties of solids. The chosen examples of experimental work are ones performed at electron synchrotron facilities, and include the use of polarization analysis, spectroscopy, Bragg scattering and dichroism.



## 1. Introduction

Magnetic photon scattering attracted the interest of theoreticians about forty years ago. However, the exploitation of the magnetic interaction in studies of condensed matter and materials research has grown rapidly in recent years following the development of both photon factories, based on electron synchrotrons that provide intense beams, and photon optical elements. Intense beams are useful because the magnetic interaction is weak, being a relativistic correction to the usually dominant charge process.

In this brief survey we aim to bring together physical ideas and theoretical concepts underlying the phenomena of photon scattering by magnetic solids, with reference to some related recent experimental work. Photon polarization effects, diffraction, spectroscopy, dichroism and elastic resonant scattering are all mentioned.

We start by discussing the basic physical ideas underlying the scattering of photons from atomic systems. The role of photon polarization in determining the outcome of a scattering measurement is explained in Section 3 and the expression for the cross section including contributions from charge and magnetic terms (spin and orbital) is presented. Photon diffraction studies and the possibility of observing the magnetic scattering amplitude is covered in Section 4, while inelastic scattering using high energy photons (Compton limit) is discussed in Section 5. Dichroism and elastic resonant scattering are outlined in Sections 6,7, respectively. Lastly, overall conclusions about magnetic photon scattering techniques are drawn together in Section 8.

Introductions to the basic elements of photon scattering are found in the books by Weissbluth (1989), and Hayes, Loudon (1978).

## 2. Essential Aspects of Photon Scattering

The classical elastic scattering of a high frequency photon by a free electron is described by the Thomson amplitude, which depends only on the charge and mass of the scattering particle. The scattering of long wavelength radiation is relatively weak, compared to the

Thomson limit, provided it is not tuned to an atomic resonance. The cross-section at resonance is of the order of the square of the wavelength and independent of the fine structure constant, so it can be relatively very large (see Section 7). Interesting phenomena appear in inelastic processes as the energy of the primary photon increases to the stage where the photon wavelength becomes comparable with or smaller than the dimension of an atom. When the primary photon energy is large compared to the atomic ionization energy ( $I$ ), transitions to states in the continuum spectrum of the atom dominate. The process becomes close to the special situation of scattering by a free electron. Momentum conservation, that is always satisfied in the free electron case, results in an intense narrow line in the scattering spectrum, centered at the recoil energy. An observed breadth in this narrow (Compton) line is determined by the momentum distribution of the initial bound state. In conclusion, in the two extremes  $\hbar\omega \ll I$  and  $\hbar\omega \gg I$  the spectrum is dominated by single lines centered at  $\omega=0$  and  $\omega = \text{free particle recoil energy}$ , respectively. The basic structure of a Compton profile is sketched in Fig.1

### 3. Photon Polarization Effects and Cross-section

The scattering cross section depends on the polarization of the primary radiation. In this section we explore some of the consequences of this dependence. Although several polarization effects are adequately treated by elementary methods, described in standard texts, slightly more formalism is required to provide a complete description of polarization contributions to the cross section and secondary beam. Fortunately, it is possible to derive master formulae that encompass all possible events. This applies to both the cross-section and the state of polarization of the secondary beam. Here, we aim to provide something of a user's guide, and hence omit derivations; see, for example, Balcar, Lovesey (1989) and Berestetskii, Lifshitz, Pitaevskii (1982).

In general, it is convenient to describe the partial polarization by means of three real Stokes parameters  $\mathbf{P}=(P_1, P_2, P_3)$ . The density matrix  $\mu$ , which describes the incident photon beam, can be written

$$\mu = \frac{1}{2} \begin{pmatrix} 1+P_3 & P_1-iP_2 \\ P_1+iP_2 & 1-P_3 \end{pmatrix} = \frac{1}{2} \{I+P \cdot \sigma\} \quad (3.1)$$

where,  $I$  is the unit matrix and  $\sigma$  are the Pauli matrices. Referring to the physical significance of  $\mu$ , one can show that the parameter  $P_3$  defines the linear polarization along the  $\xi$ - and  $\eta$ -axis, defined in Fig. 2. The value  $P_3 = 1$  corresponds to complete polarization perpendicular to the scattering plane, often called  $\sigma$ -polarization, and  $P_3 = -1$  is complete polarization in the scattering plane, often called  $\pi$ -polarization. The parameter  $P_2$  represents the degree of circular polarization. The probability of right-handed polarization is  $(1+P_2)/2$ , and of left-hand polarization is  $(1-P_2)/2$ . Since these two polarizations correspond to helicities  $\pm 1$ , it is clear that  $P_2$  is the mean value of the photon helicity. One can show that  $P_1$  provides the linear polarization along directions at angles  $\pm\pi/4$  to the  $\xi$ -axis. Complete linear polarization is described by  $P_2 = 0$ ,  $P_1^2 + P_3^2 = 1$ , the unpolarized state by  $P_1 = P_2 = P_3 = 0$ , and the completely polarized state by  $P_1^2 + P_2^2 + P_3^2 = 1$ .

The scattering amplitude operator  $G$  is written as a 2x2 matrix with respect to the polarization of the primary and the secondary photon states,

$$\mathbf{G} \equiv \begin{pmatrix} G_{\sigma\sigma} & G_{\sigma\pi} \\ G_{\pi\sigma} & G_{\pi\pi} \end{pmatrix} \equiv \begin{pmatrix} \beta + \alpha_3 & \alpha_1 - i\alpha_2 \\ \alpha_1 + i\alpha_2 & \beta - \alpha_3 \end{pmatrix} \quad (3.2)$$

where  $\beta$  is a scalar operator and  $\alpha$  a vector operator. The cross section is then given by,

$$\frac{d\sigma}{d\Omega} = r_e^2 \left( \frac{q'}{q} \right) \text{Tr}(\mu \mathbf{G} \cdot \mathbf{G}) \quad (3.3)$$

where,  $r_e \sim 0.3 \times 10^{-12} \text{ cm}^{-1}$  is the classical radius of an electron, and the Stokes vector for the secondary photon

$$\left( \frac{d\sigma}{d\Omega} \right) \mathbf{P}' = r_e^2 \left( \frac{q'}{q} \right) \text{Tr}(\mu \mathbf{G} \cdot \sigma \mathbf{G}). \quad (3.4)$$

The trace operation in (3.4) is taken with respect to the photon polarization states. Inserting the expressions (3.1) and (3.2) in (3.3) and (3.4) and performing the trace operation leads to the master formulae for the cross section :

$$\frac{d\sigma}{d\Omega} = r_e^2 \left(\frac{q'}{q}\right) \left[ \alpha^+ \cdot \alpha + \beta^+ \beta + \beta^+ (\alpha \cdot \mathbf{P}) + (\alpha^+ \cdot \mathbf{P}) \beta + i \mathbf{P} \cdot (\alpha^+ \times \alpha) \right], \quad (3.5)$$

and the secondary polarization :

$$\begin{aligned} \left(\frac{d\sigma}{d\Omega}\right) \mathbf{P}' = r_e^2 \left(\frac{q'}{q}\right) & \left[ \beta^+ \alpha + \alpha^+ \beta - i(\alpha^+ \times \alpha) + \beta^+ \beta \mathbf{P} + \alpha^+ (\alpha \cdot \mathbf{P}) + (\alpha^+ \cdot \mathbf{P}) \alpha \right. \\ & \left. - \mathbf{P} (\alpha^+ \cdot \alpha) + i \beta^+ (\alpha \times \mathbf{P}) + i (\mathbf{P} \times \alpha^+) \beta \right]. \end{aligned} \quad (3.6)$$

Eqns (3.5) and (3.6) provide general statements with regard to the polarization dependence of the cross section and the polarization of the secondary beam. To obtain results for the interpretation of experiments (Bragg diffraction, Compton scattering, resonant scattering, etc.) appropriate matrix elements of the operators  $\alpha$  and  $\beta$  are formed. It is understood in (3.5) and (3.6) that there is conservation of energy in the scattering process, and this is made explicit in subsequent formulae.

Consider a scattering process, depicted in Fig. 2, during which a primary photon  $q$  with energy  $E$  and polarization  $\epsilon$  is scattered to a photon  $q'$ ,  $E'$ ,  $\epsilon'$  by an assembly of charged particles described by the Hamiltonian  $H$  and initially in a state  $\mu$  with energy  $E_\mu$ . This process involves all particles with the radiation field, and the interaction of their spins with the magnetic component of the field. The corresponding dimensionless scattering amplitude operator reads,

$$\begin{aligned} \mathbf{G} = \epsilon \cdot \epsilon' \mathbf{n}(\mathbf{k}) + \frac{i}{2} \tau \left(1 + \frac{q'}{q}\right) \mathbf{S}(\mathbf{k}) \cdot (\epsilon \times \epsilon') + \\ + \left(\frac{1}{m}\right) \left\{ \epsilon' \cdot \mathbf{J}(-q') \left[E_\mu + E - H\right]^{-1} \epsilon \cdot \mathbf{J}(q) + \epsilon \cdot \mathbf{J}(q) \left[E_\mu - E' - H\right]^{-1} \epsilon' \cdot \mathbf{J}(-q') \right\}, \end{aligned} \quad (3.7)$$

where the momentum transfer  $\mathbf{k}=\mathbf{q}-\mathbf{q}'$ , and  $\tau=(\hbar q/mc)$ . Expression (3.7) is correct to first order in  $\tau$  (Grotch et al. 1983). The Fourier transforms of the current density, charge density and spin density operators are defined by,

$$\mathbf{J}(\mathbf{q}) = \sum_j (\mathbf{p}_j + i\hbar \mathbf{s}_j \times \mathbf{q}) \exp(i\mathbf{q} \cdot \mathbf{R}_j), \quad (3.8)$$

$$n(\mathbf{k}) = \sum_j \exp(i\mathbf{k} \cdot \mathbf{R}_j), \quad (3.9)$$

$$\mathbf{S}(\mathbf{k}) = \sum_j \mathbf{s}_j \exp(i\mathbf{k} \cdot \mathbf{R}_j), \quad (3.10)$$

and the summation is understood over all charged particles (electrons).

When  $E, E'$  are much in excess of the energies of states in the spectrum of  $H$  (Compton limit), the resolvent operators in (3.7) can be safely expanded in  $(1/E)$  and  $(1/E')$ . After some algebra one obtains the following non-resonant expression for the scattering amplitude operator,

$$\mathbf{G} = \boldsymbol{\varepsilon}' \cdot \boldsymbol{\varepsilon} n(\mathbf{k}) - i\tau[\mathbf{S}(\mathbf{k}) \cdot \boldsymbol{\mathcal{B}} + \mathbf{Z}(\mathbf{k}) \cdot \boldsymbol{\mathcal{A}}] \quad (3.11)$$

with

$$\boldsymbol{\mathcal{A}} = \boldsymbol{\varepsilon}' \times \boldsymbol{\varepsilon} = \begin{pmatrix} 0 & \hat{\mathbf{q}} \\ -\hat{\mathbf{q}}' & \hat{\mathbf{q}}' \times \hat{\mathbf{q}} \end{pmatrix}. \quad (3.12a)$$

$$\begin{aligned} \boldsymbol{\mathcal{B}} &= \frac{1}{2} \left(1 + \frac{q'}{q}\right) [\boldsymbol{\varepsilon}' \times \boldsymbol{\varepsilon} - (\hat{\mathbf{q}}' \times \boldsymbol{\varepsilon}') \times (\hat{\mathbf{q}} \times \boldsymbol{\varepsilon})] + \left(\frac{q'}{q}\right) (\hat{\mathbf{q}} \cdot \boldsymbol{\varepsilon}) (\hat{\mathbf{q}}' \times \boldsymbol{\varepsilon}') - (\hat{\mathbf{q}} \cdot \boldsymbol{\varepsilon}') (\hat{\mathbf{q}} \times \boldsymbol{\varepsilon}) \\ &= \begin{pmatrix} a(\hat{\mathbf{q}} \times \hat{\mathbf{q}}') & (a-b)\hat{\mathbf{q}} + (b\cos\theta - a)\hat{\mathbf{q}}' \\ (a - \cos\theta)\hat{\mathbf{q}} + (1-a)\hat{\mathbf{q}}' & (b+1-a)(\hat{\mathbf{q}} \times \hat{\mathbf{q}}') \end{pmatrix}; \end{aligned} \quad (3.12b)$$

here,  $b=q/q'$ ,  $a=(1+b)/2$ ,  $\cos\theta=\hat{\mathbf{q}} \cdot \hat{\mathbf{q}}'$ , and

$$\boldsymbol{\varepsilon}' \cdot \boldsymbol{\varepsilon} = \begin{pmatrix} 1 & 0 \\ 0 & \hat{\mathbf{q}} \cdot \hat{\mathbf{q}}' \end{pmatrix}. \quad (3.12c)$$

The dimensionless operator  $Z(\mathbf{k})$  that occurs in (3.11) is defined as,

$$\mathbf{Z}(\mathbf{k}) = \frac{i}{\hbar q} \sum_j \exp(i\mathbf{k} \cdot \mathbf{R}_j) (\hat{\mathbf{q}} - \hat{\mathbf{q}}') \times \mathbf{p}_j \quad (3.13)$$

and it can be shown that it is proportional to the orbital magnetization of the target assembly (Balcar, Lovesey 1989). Notice that the photon interaction contains the same microscopic densities as the magnetic neutron interaction. However, in contrast to the neutron case, the weights of the two magnetic densities differ and depend on the initial and final photon wave vectors. This affords the possibility of observing separately the spin and current (or orbital) densities (Balcar, Lovesey 1989, and Lander, Stirling 1992).

Employing the definitions of the physical quantities entering the scattering amplitude operator one can derive the following expressions for the operators  $\alpha_1, \alpha_2, \alpha_3, \beta$ , defined in (3.2),

$$\alpha_1 = -\frac{i}{2} \tau \mathbf{S}(\mathbf{k}) \cdot \{(2a - b - \cos\theta)\hat{\mathbf{q}} + (1 - 2a + b\cos\theta)\hat{\mathbf{q}}'\} - \frac{i}{2} \tau (\hat{\mathbf{q}} - \hat{\mathbf{q}}') \cdot \mathbf{Z}(\mathbf{k}) \quad (3.14a)$$

$$\alpha_2 = \frac{i}{2} \tau \mathbf{S}(\mathbf{k}) \cdot \{(\cos\theta - b)\hat{\mathbf{q}} + (b\cos\theta - 1)\hat{\mathbf{q}}'\} + \frac{i}{2} \tau (\hat{\mathbf{q}} + \hat{\mathbf{q}}') \cdot \mathbf{Z}(\mathbf{k}) \quad (3.14b)$$

$$\alpha_3 = \frac{i}{2} (1 - \cos\theta) n(\mathbf{k}) + \frac{i}{2} \tau (\hat{\mathbf{q}} \times \hat{\mathbf{q}}') \cdot \{(b + 1 - 2a)\mathbf{S}(\mathbf{k}) - \mathbf{Z}(\mathbf{k})\} \quad (3.14c)$$

$$\beta = \frac{i}{2} (1 + \cos\theta) n(\mathbf{k}) + \frac{i}{2} \tau (\hat{\mathbf{q}} \times \hat{\mathbf{q}}') \cdot \{\mathbf{Z}(\mathbf{k}) - (b + 1)\mathbf{S}(\mathbf{k})\}, \quad (3.14d)$$

Notice that  $\alpha_1$  and  $\alpha_2$  are purely magnetic in character ( $\alpha_1 = \alpha_2 = 0$  for  $\tau = 0$ ), while  $\beta$  contain both magnetic and charge terms. It is worth mentioning that the charge and magnetic terms in  $\alpha_3$ , and  $\beta$ , differ by a phase factor  $i$ . Lastly, the above expressions are correct to first order in  $\tau$ . Equations (3.5), (3.6) and (3.15) constitute the theoretical basis for studying non-resonant, elastic or inelastic photon scattering.

#### 4. Diffraction

Consider the cross section (3.5). Assume, in the first instance, that the matrix elements of the atomic quantities  $n(\mathbf{k})$ ,  $\mathbf{S}(\mathbf{k})$  and  $\mathbf{Z}(\mathbf{k})$  are purely real, which is, for example, the case for a centrosymmetric target sample. Assume also that the incident energy is well away from

a resonance for any atom in the target. Then, the cross section for diffraction, which is proportional to  $|\langle\alpha\rangle|^2 + |\langle\beta\rangle|^2$ , contains charge terms of order  $\tau^0$  and purely magnetic terms of order  $\tau^2$ . The latter are many orders of magnitude smaller than the former (as  $\tau \ll 1$ ), and consequently the magnetic content of a Bragg reflection is dominated by the charge contribution. However, purely magnetic reflections can be observed in magnetic materials for which the magnetic structure shows a superperiodicity with respect to the underlying chemical structure. Such observations have been made in the pioneering experiments of Brunel, de Bergevin (1981) on antiferromagnetic NiO (see the review by de Bergevin, Brunel 1986) and helimagnets like holmium (Gibbs et al. 1985).

If, however, the matrix elements  $\langle\alpha\rangle$  and  $\langle\beta\rangle$  possess imaginary charge components (eg non-centrosymmetric materials, or resonance conditions), then the cross section contains terms proportional to  $\tau$ , that are probably larger than the purely magnetic terms. A study of rare earth multilayers (Vettier et al. 1986) revealed a term linear in the magnetic amplitude that was generated by an imaginary component in the charge amplitude, achieved by tuning the wavelength to an atomic resonance.

The relative polarization of the primary and secondary beams has a significant effect on the cross section. The polarization factors  $A$  and  $B$  contain off-diagonal elements, while the  $(\epsilon' \cdot \epsilon)$  factor is purely diagonal. This means that detecting a secondary beam with a linear polarization perpendicular to the primary beam,  $(\sigma-\pi)$  or  $(\pi-\sigma)$  events, will isolate the purely magnetic scattering events. The observation by Gibbs et al. (1985) of the effect of the crystal field perturbation on the orientation of magnetic moments in metallic holmium, Fig.(3), shows a diffraction pattern, obtained with a polarised analyser that allows isolation of  $(\sigma-\pi)$  events.

Beams with circular polarization have played a crucial rôle in revealing the magnetic component of the cross section. This is because, for real matrix elements  $\langle\alpha\rangle$  and  $\langle\beta\rangle$ , the phase difference between their charge and magnetic components is negated by the imaginary part of the complex polarization vectors leading to purely real interference terms, which are of order  $\tau$ . The sign of the interference terms changes with the polarity of the polarization

affords to the appealing possibility of a difference measurement to isolate the relatively small linear magnetization contribution. This scheme has value only for materials with mixed (charge and magnetic) Bragg reflections, as in a simple ferromagnet. Magnetic diffraction from ferromagnetic iron of circularly polarized photons has been reported by Collins, Laundy, Rollanson (1992). They used, for the first time, a white beam and single crystal sample, and reversed the direction of magnetization by an applied magnetic field to affect isolation of the polarization induced charge-magnetic interference contribution.

One can show that a scattering geometry can be chosen at which the magnetic scattering is either purely orbital or spin in nature. This is a possibility not available in neutron scattering (Lander, Stirling 1992). A separate measurement of spin and orbital contributions to magnetic scattering has first been realized by Gibbs et al. (1991) in their study of holmium metal.

Finally, we mention the impressively high resolution in reciprocal lattice space obtainable in diffraction studies using photon beams generated by synchrotron sources (Bohr, et al. 1989, and Bohr, Gibbs, Huang 1990).

## 5. Spectroscopy

With the term spectroscopy one refers to non-resonant inelastic scattering events. Events involving low energy collective excitations (phonons, plasmons) of the target system and interband electronic transitions are reviewed Burkel (1991). Experiments on light scattering by spin waves in ordered magnets are reviewed by Cottam, Lockwood (1986). The interpretation uses the modulation of the target's permittivity by spin waves, and not the weaker magnetic dipole interaction between spin fluctuations and the magnetic vector of the light. For our part, the interest is in the high energy, Compton limit of the spectrum probed by hard X-rays.

Charge distributions in solids have been studied with hard X-rays ( $\sim 40\text{keV}$ ) and the results have been analysed in terms of the first term of the scattering operator (3.7), that is valid in the Compton limit ( $E, E' \gg I$ ). The subject is reviewed by Cooper (1985). Platzman,

Tzoar (1965) and Grotch, Kazes, Bhatt, Owen (1983) have developed the theory of spin-dependent Compton scattering from bound electron. Currently, one topic of experimental and theoretical interest is interference between charge and magnetic (orbital) amplitudes. This interference is induced by circular polarization of the primary beam, and it is analogous to the mixed charge-magnetic Bragg reflection mentioned in the previous section.

Cooper et al. (1992) after careful studies to detect the possible presence in Compton scattering data of a contribution from orbital magnetism, reached a negative conclusion. Lovesey (1993) gave support to the findings by Cooper et al. (1992), using a simplified model for the Compton limit, in which the final electron state was simply approximated by a plane wave.

Further calculations (Trohidou, Kechrakos, Lovesey 1993), including the corrections to the plane wave state arising from the requirement of orthogonality to the initial bound state, have produced a non-zero contribution to the interference cross-section. This is proportional to the product of the overlap integral between the initial (bound) state with the plane wave and the angular momentum of the initial electron state. Consequently, the interference cross-section is vanishingly small in the limit  $E' \gg I$ . A similar conclusion has been reached in numerical calculations using the hydrogen atom as a model atomic system.

## 6. Elastic Resonant Scattering

When the incident photon energy is near the absorption edge, large resonant scattering is observed. The cross section depends on the specific absorption edge, photon polarization states, and the magnetic state of the sample. The latter feature makes resonant scattering a useful technique for the study of magnetic materials. The largest resonant enhancement has been observed for incident photon energies near the  $M_4$  absorption edges in actinides, and near the  $L_3$  absorption edges in rare earth and transition metals. The first observation of magnetic resonant scattering was reported by Gibbs et al. (1988) in a study of the magnetic spiral structure of metallic holmium. An interpretation in terms of electric multipole transitions has been provided by Hannon, Trammell, Blume, Gibbs (1988).

The total amplitude for coherent elastic scattering by photons is the sum of pure charge, pure non-resonant magnetic contributions and a contribution from dispersive and absorptive processes. The latter contain both charge and magnetic interactions. In the experiments reported to date the observed intensities and polarization dependence are accounted for by the charge contribution to the resonant processes. In this case the magnetic character of the scattering arises from the magnetic character of the electronic orbitals that enter the calculation of the matrix elements of the multipole operators. For holmium, studied by Gibbs et al. (1991), the significant events are virtual dipole allowed transitions, coupling 2p core electrons to 5d - derived conduction band states, and quadrupole transitions coupling 2p core electrons to 4f - atomic like states. It is found for the spiral magnetic phase that, some magnetic satellites arise solely from quadrupole transitions, while the remaining observed satellites are mixtures of dipolar and quadrupolar transitions.

The interpretation of resonant magnetic scattering provided by Hannon, Trammell, Blume, Gibbs (1988) accounts for the observations on holmium reported by Gibbs et al. (1991) and the findings of measurements on various uranium compounds with an antiferromagnetic configuration of moments (McWhan et al. 1990, Tang et al. 1992). Large resonant cross-sections observed at the  $M_4$  edge of U in UAs have been successfully interpreted in terms of three dipole operators that add coherently, as demonstrated by the data displayed in Fig.(4).

The observed polarization dependence of resonant scattering, satellite selection rules and basic features of line shapes are quite elementary consequences of a model based on electric multipole contributions to the resonant scattering amplitude. The outstanding calculation required to fully confirm the experimental and theoretical findings is the calculation of radial integrals which arise in matrix elements of multipole operators.

Tang et al. (1991) report ab initio atomic calculations of the resonance scattering amplitude at the  $M_4$  and  $M_5$  edges of uranium in  $UO_2(U^{4+})$  and  $USb(U^{3+})$ . Radial integrals in the calculations were obtained from a Hartree-Fock scheme, including relativistic corrections. Fits to the experimental data are good for  $UO_2$ , modelled by  $U^{4+}$ , indicating that an atomic picture is useful. Some discrepancies are found between experimental data and calculations for

USb, which might indicate the need to go beyond an atomic picture and include hybridization between f states and band states.

## 7. Dichroism

Spin dependent photon absorption is usually called magnetic x-ray dichroism. The relation between absorption and scattering is given by the optical theorem, which reveals a proportionality between the absorption coefficient and the imaginary part of the forward scattering amplitude. Within a simple one-electron picture of electronic structure, in resonant scattering the incident photon promotes, by a virtual transition, an inner shell electron to an unoccupied orbital above the Fermi energy, which subsequently decays through the emission of an elastically scattered photon. The amplitude of the resonant magnetic scattering depends on the matrix elements which couple the initial state and intermediate magnetic states allowed by the Pauli exclusion principle. We recall that the scattering amplitude contains charge, linear momentum and magnetic interaction operators. To date, the experimental data on resonant scattering and dichroism have been successfully interpreted in terms of matrix elements of the momentum interaction operator. The magnetic character of the observed electron-photon events in magnetic materials stems entirely from the nature of the wave functions used to calculate the dipole, quadrupole, etc. matrix elements.

To get the basic physical picture, consider the schematic atomic energy level diagram displayed in Fig.(5). Only K and L core atomic initial states are indicated together with some higher, partially filled intermediate states. If photoabsorption proceeds through the dipole operator, the selection rule for the initial( $l$ ) and the final ( $l'$ ) orbital angular momentum is  $l'=l\pm 1$ . Thus for the case of photoabsorption by a  $2p_{3/2}$ , depicted in Fig.(5), separated in energy from  $2p_{1/2}$  primarily by the spin-orbit interaction, the final spin-down states are of d-like character.

Magnetic dichroism is measured by detecting the difference of the absorption coefficient of circularly polarized photons for parallel and antiparallel orientation of the photon spin and the net moment of the absorber. The matrix elements in the absorption coefficient depend on

the initial and final state spin-orbit configurations. Very strong dichroism effects have been observed in the 3d-4f absorption spectra of rare-earth materials.

Experimental data and theoretical results for Gd  $L_1$ ,  $L_2$  and  $L_3$  absorption, and corresponding spin-dependent profiles, are shown in Fig.(6). The calculations are based on a single-band model and they account for the experimental data on the  $L_1$ ,  $L_2$ ,  $L_3$  edges absorption for positive energies. The experimental  $L_2$ ,  $L_3$  spectra show a significant decrease of the signal at the lower energy side, especially for the  $L_3$  edge. It has been proposed (Carra et al. 1991) that the discrepancy can be accounted for by atomic quadrupole transitions to empty 4f states, which in the case of Gd are negative spin polarized.

## 8. Conclusions

Photon scattering has been shown to have significant potential for the study of magnetic properties of materials. The very high wave vector resolutions can provide information not readily obtained by neutron diffraction measurements. Another attractive feature is the sensitivity of resonant scattering to the atomic species. Photon resonant scattering can access high order multipole events. Magnetic circular dichroism has been applied to a wide variety of systems including transition metals, surfaces, thin-films, rare-earth compounds and biological samples. Several experimental studies have already demonstrated the value of the polarization dependence of magnetic photon scattering.

While there has been experimental activity in the past few years, a comparison with the history of developments of neutron beam techniques to study magnetic material, supports the view that it might be another decade before photon beam techniques can be placed in proper context with established techniques.

**Acknowledgements** We thank the following researchers for use of diagrams from their published work: G. Schütz, D. B. McWhan, and D. Gibbs.

The review contributes to an EC funded twinning project financed through contract No. SCI 0467.

## References

Balcar, E., Lovesey, S.W.: Theory of magnetic neutron and photon scattering, Oxford University Press 1989

Berestetskii, V.G., Lifshitz, E.M., Pitaevskii, L.P.: Quantum electrodynamics, Vol. 4 Course of Theoretical Physics. Oxford: Pergamon Press 1982.

de Bergevin, F., Brunel, M.: Acta Crystallogr. **A37** (1981) 314

de Bergevin, F., Brunel, M.: in Structure and Dynamics of Molecular Systems, Vol.2, (Eds. R.Daudel et al), New York : Reidel 1986.

Bohr, J., Gibbs, D., Axe, J.D., Moncton, D.E., D'Amico, K.L., Majkrzak, C.F., Kwo, J., Hong, M., Chien, C.L., Jensen, J.: Physica **B159** (1989) 93

Bohr, J., Gibbs, D., Huang, K.: Phys.Rev. **B42** (1990) 4322

Burkel, E.: Inelastic Scattering of X-rays with very high energy resolution, Berlin: Springer-Verlag 1991

Carra, P., Harmon, B.N., Thole, B.T., Altarelli, M., Sawatzky, G.A., Phys.Rev.Lett. **66** (1991) 2495

Collins, S.P., Laundry, D., Rollanson, A.J.: Phil.Mag. **B65** (1992) 37

Cooper, M.J.: Rep.Prog.Phys. **48** (1985) 415

Cooper, M.J., Zukowski, E., Collins, S.P., Timms, D.N., Hoh, F., Sakurai, H.: J.Phys.:Cond.matter. **4** (1992) L399

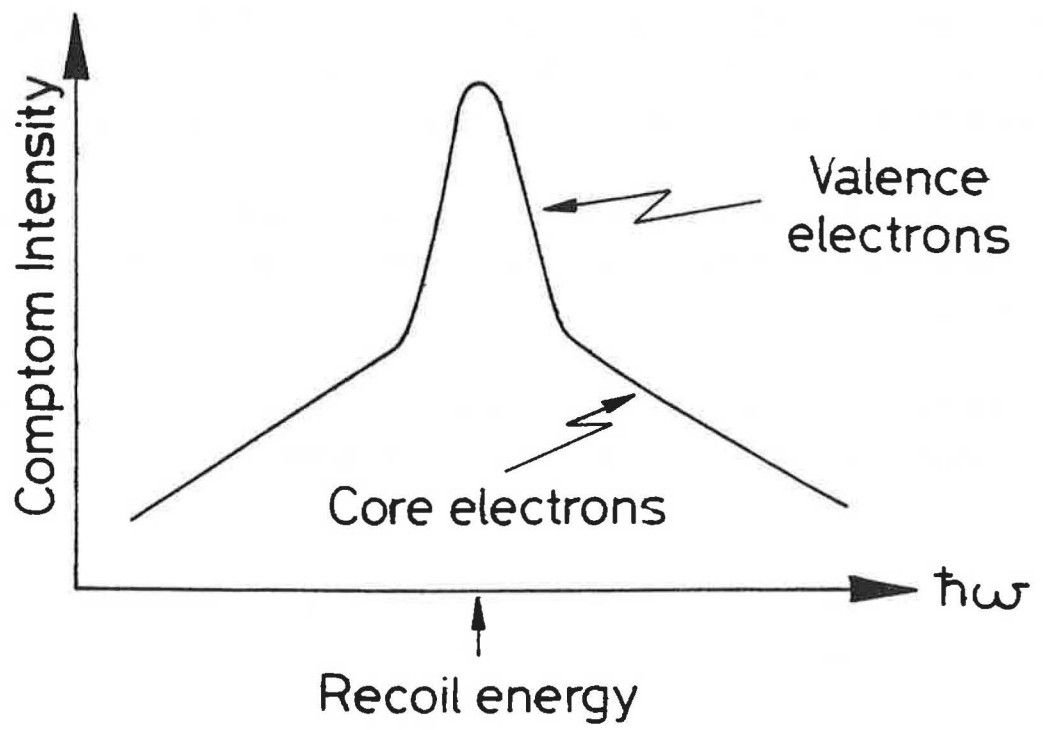
Cottam, M.G., Lockwood, D.J.: Light scattering in magnetic solids. New York: John Wiley 1986.

Gibbs, D., Grubel, G., Harshnan, D.R., Isaacs, E.D., McWhan, D.B., Mills, D., Vettier, C.: Phys.Rev. **B43** (1991) 5663

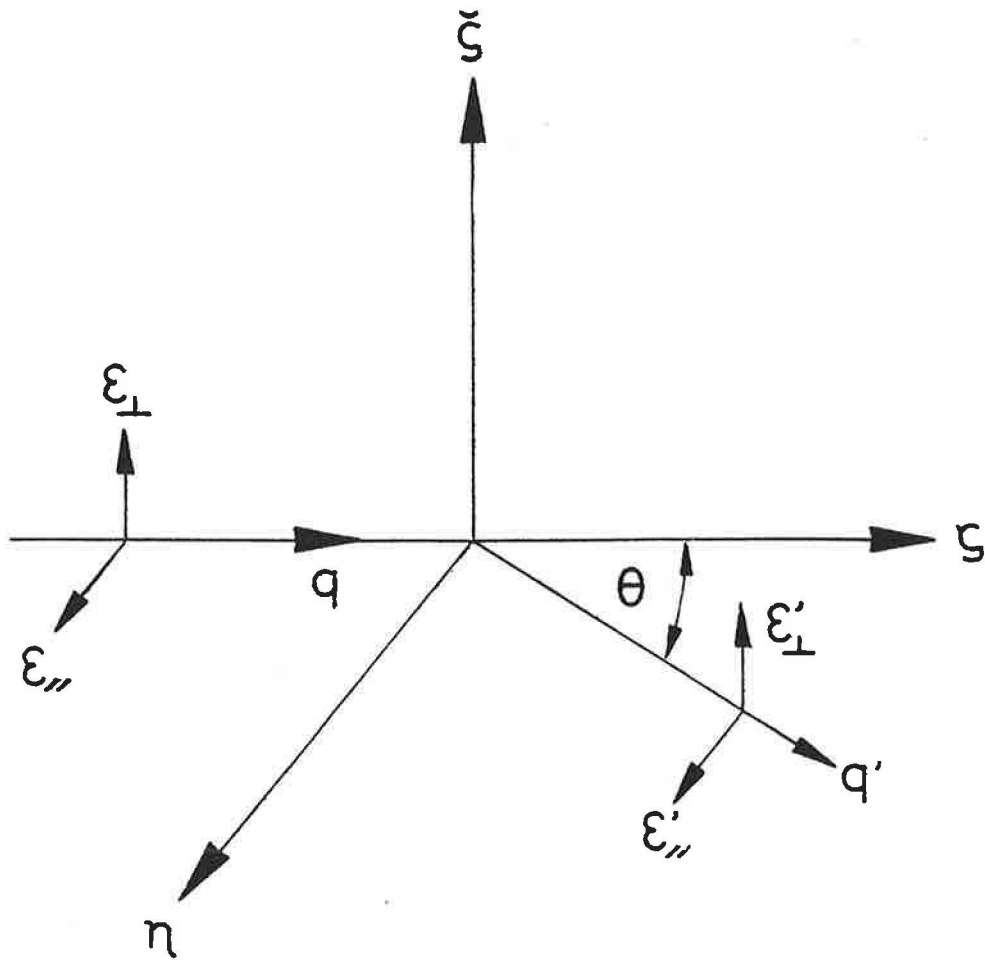
- Gibbs, D., Harshman, D.R., Isaacs, E.D., McWhan, D.B., Mills, D., Vettier, C.: Phys.Rev.Lett. 61 (1988) 1241
- Gibbs, D., Moncton, D.E., D'Amico, K.L., Bohr, J., Grier, B.H.: Phys.Rev.Lett. 55 (1985) 234
- Grotch, H., Kazes, E., Bhatt, G., Owen, D.A.: Phys.Rev. **A27** (1983) 243
- Hannon, J.P., Trammell, G.T., Blume, M., Gibbs, D.: Phys.Rev.Lett. 61 (1988) 1245; ibid 62 (1989) 2644(E)
- Hayes, W., Loudon, R.: Scattering of light by crystals. New York: John Wiley 1978.
- Lander, G.H., Stirling, W.G.: Phys.Scripta, **T45** (1992) 15
- Lovesey, S.W.: Rep.Prog.Phys. 56 (1993) 257
- McWhan, D.B., Vettier, C., Isaacs, E.D., Ice, G.E., Siddons, D.P., Hastings, J.B., Peters, C.: Vogt, O., Phys.Rev. 42 (1990) 6007
- Platzman, P.M., Tzoar, N.: Phys.Rev. **A139** (1965) 140
- Schütz, G.: Magnetic X-ray Scattering (Proc. Daresbury Study Weekend) eds. Stirling, W.G., Cooper, M.J. and Pattison, P. (SERC Daresbury Laboratory Report DL/SCI/R30)
- Tang, C.C., Stirling, W.G., Lander, G.H., Gibbs, D., Herzog, W., Carra, P., Mattenberger, K., Vogt, O.: Phys.Rev. **B46** (1992) 5287
- Trohidou, K.N., Kechrakos, D., Lovesey, S.W.: (1993)
- Vettier, C., McWhan, D.B., Gyorgy, E.M., Kwo, J., Buntschuh, B.M., Batterman, B.W.: Phys.Rev.Lett. 56 (1986) 757
- Wesibluh, M.: Photon-Atom Interactions. Boston: Academic Press 1989.

## Figure Captions

- (1) The two basic contributions to the Compton intensity are illustrated. The core and valence electron contributions are distinguished by the size of the Doppler broadening
- (2) Coordinates  $\xi, \eta, \zeta$  are illustrated. The  $\xi$  axis is perpendicular to the plane of scattering defined by the primary and secondary photon wave vectors  $q$  and  $q'$ ,  $k=q-q'$ , and  $\theta$  is the scattering angle. It is common practice to label  $\epsilon_{\perp}$  and  $\epsilon_{\perp}'$  as  $\sigma$ -polarisation states, and  $\epsilon_{\parallel}$  and  $\epsilon_{\parallel}'$  as  $\pi$ -polarisation states.
- (3) Two satellites observed in scattering from holmium at 17K. The filter isolates ( $\sigma$ - $\pi$ ) events which are purely magnetic. (After Gibbs et al. 1985).
- (4) The energy dependence of the intensity at a satellite in UAs through the  $M_5$ ,  $M_4$  and  $M_3$  absorption edges. The solid line through the data is a fit to the coherent sum of three dipole oscillators. Inset is an expanded view of the  $M_3$  edge. (After McWhan et al. 1990)
- (5) An illustration of electron states engaged in dichroism; only a few core states are displayed, and the conduction bands are shown without the rich structure that exists in results from a realistic model.
- (6) Experimental (dashed line) and theoretical (solid line) absorption and corresponding absorption coefficient for  $L_1$ ,  $L_2$  and  $L_3$  edges of gadolinium metal. (After Schütz 1991)



^



(2)

